Denoising of MRI Images Using Curvelet Transform

Ranjit Biswas, Debraj Purkayastha and Sudipta Roy

Abstract Most of the medical images are usually affected by different types of noises during acquisition, storage, and transmission. These images need to be free from noise for better diagnosis, decision, and results. Thus, denoising technique plays an important role in medical image analysis. This paper presents a method of noise removal for brain magnetic resonance imaging (MRI) image using curvelet transform thresholding technique combined with the Wiener filter and compares the result with the curvelet and wavelet-based denoising techniques. To assess the quality of denoised image, the values of peak signal-to-noise ratio (PSNR), mean square error (MSE), and structural similarity index measure (SSIM) are considered. The experimental results show that curvelet denoising method depicts better result than wavelet denoising method, but the combined method of curvelet with Wiener filtering technique is more effective than the wavelet- and curvelet-based denoising method in terms of PSNR, MSE, and SSIM.

Keywords Wiener filter · Wavelet transform · Curvelet transform · Denoising

1 Introduction

Medical images are having an important role for diagnosis of diseases. These images are obtained from various methods such as MRI, CT, and X-ray imaging. Nowadays, these images are captured using digitized systems. During the

R. Biswas (✉)
Department of Information Technology, Ramkrishna Mahavidyalaya, Kailashahar, Tripura 799277, India
e-mail: ranjit_tb@yahoo.co.in

D. Purkayastha · S. Roy
Department of Computer Science & Engineering, Assam University, Silchar 788011, India
e-mail: cyberdebraj@gmail.com

S. Roy
e-mail: sudipta.it@gmail.com

A. Konkani et al. (eds.), *Advances in Systems, Control and Automation*,
Lecture Notes in Electrical Engineering 442, https://doi.org/10.1007/978-981-10-4762-6_55

acquisition process, the images may be corrupted by different types of noise and it is very important to remove the noise to get better interpretation. Removal of noise from digital images is a big challenge for the researchers. Huang et al. [1] proposed a type of median filtering technique which is much faster and was implemented in 2D. Later, Ney [2] implemented a technique of dynamic programming for implementing nonlinear smoothing filters, which gives a good result in removing noise but keeps much more information around the curves by penalizing when there is large difference in two consecutive samples and rewarding when these are close. Saluja et al. [3] proposed an adaptive Wiener filter based on wavelet transform to calculate coefficients of weighted high-pass filtering. Boulfelfel et al. [4] investigated the usage of Wiener filter and PSE filter in CT images and developed a 3D filter that performs better than 2D filters.

The transform domain filtering contains wavelet transform, ridgelet transform, and curvelet transform. Lang et al. [5] used wavelet analysis of undecimated wavelet transform on unidimensional signals to remove noise which was one of the earlier implementations of wavelet in noise removal. To remove noise and to compress image, Chang et al. [6] used adaptive wavelet soft threshold using data-driven method called as Bayes Shrink method for threshold estimation. Mojsilovic et al. [7] classified the stages of liver disease using wavelet transform. One of the important thresholding techniques—Visu Shrink developed by Donoho et al. [8, 9] using wavelet shrinkage. Another technique called SURE (Stein's Unbiased Risk Estimator) shrink also developed by Donoho et al. [10], which is based on SURE estimator developed by Steinin [11]. Stein name it as Unbiased Risk Estimator. SURE estimator estimates mean of random normal variable which is independent. Zhang [12] proposed and implemented diffusion in image domain and also in wavelet domain.

Candes and Donoho [13] showed ridgelet transform of images. Based on ridgelets, curvelet transform came into existence. The disadvantage of wavelet denoising is that it does not perform well while denoising in the curves in an image and results in loss of details. Starck and Candes in [14] proposed a curvelet transform based on Candes's ridgelet technique. This technique can efficiently represent a curve because it has ability to select and identify curves along with time and frequency relations. This technique also uses wavelet shrinkage for thresholding. Ulfarsson et al. [15] removed speckle noise efficiently from SAR images using curvelet domain transform. Liu et al. [16] studied and analysed the curvelet based on ridgelet. Ali et al. [17] developed a method to fuse CT image and MR image, and the fusion is done in curvelet domain.

2 Denoising Techniques

There are two fundamental approaches to image denoising, viz. spatial domain filtering and transform domain filtering methods.

2.1 Wavelet Transform

Wavelet is very useful for nonlinear representation of signals. Wavelet basically decomposes the image into its time and frequency relation components. Thus, the image is transformed into frequencies rather than pixel. In the wavelet domain, the noisy image is decomposed into four subsamples according to their low (L) and high (H) frequency bands called LL, LH, HL, and HH. The LL subsample is again decomposed into four subsamples at level two [3] and so on as per the requirement of the computation.

2.2 Curvelet Transform

Stark and Candes [14] solved the problem of wavelet transform by proposing curvelet transform based on ridgelet transform. Ridgelet implementation was done by converting it into radon transform. In the ridgelet transform, support interval or the scaling is done by anisotropy scaling relationship, denoted by Eq. (1).

$$\text{width} = \text{length}^2 \tag{1}$$

This was done in the first generation of curvelet transform using multiscaling ridgelet where the curve is divided into blocks and the subblocks are approximated into a straight line and ridgelet analysis is done upon it. The basic curvelet decomposition steps are given as follows.

The subband decomposition is done by Eq. (2).

$$f \mapsto (P_0 f, \Delta_1 f, \Delta_2 f, \ldots) \tag{2}$$

where P_0 are subband filters, and $\Delta_s, s \geq 0$, and subbands $\Delta_s f$ contain details about 2^{-2s} wide. The smooth windows are $w_Q(x_1, x_2)$ which are localized in diadic squares and which is defined by Eq. (3).

$$Q = [k_1/2^s, (k_1+1)/2^s] \times [k_2/2^s, (k_2+1)/2^s] \tag{3}$$

Then, the resulting square is renormalized to unit scale, which is represented by Eq. (4).

$$g_Q = T_Q^{-1}(w_Q \Delta_S f), \quad Q \in Q_S \tag{4}$$

where $(T_Q f)(x_1, x_2) = 2^s f(2^s x_1 - k_1, 2^s x_2 - k_2)$ is a renormalization operator.

After the renormalization, the ridgelet transform is done by Eq. (5).

$$\alpha_{\mu} = \langle g_Q, p_\lambda \rangle \tag{5}$$

3 Thresholding Technique

Thresholding in transform domain is achieved by hard thresholding and soft thresholding to remove unwanted noise signals. Hard thresholding removes all the value after a certain limit, and soft thresholding lowers the intensity of noise towards zero values, which is defined by Eqs. (6) and (7).

$$y(t)_{\text{Hard}} = \begin{cases} x(t) & |x(t)| \geq T \\ 0 & |x(t)| < T \end{cases} \tag{6}$$

$$y(t)_{\text{Soft}} = \begin{cases} \text{sign}(x(t)) \cdot (|x(t)| - T) & |x(t)| \geq T \\ 0 & |x(t)| < T \end{cases} \tag{7}$$

where T is threshold value, and x and y are input and output coefficients in the respective transform domain.

The threshold value in wavelet domain is calculated by Donoho et al. [10], using Visu Shrink method. Visu Shrink is based on universal thresholding as explained in the following Eq. (8).

$$T_w = \sigma\sqrt{\log(N)} \tag{8}$$

where T is the threshold value, N is the size of image, and ∂ is the noise variance.

The threshold value in curvelet transform is calculated by value of 3*sigma and 4*sigma [18] used for the coarse-scale and fine-scale elements (9).

$$T_c = 3 * \text{sigma} + \text{sigma} * (s == \text{length}(C)) \tag{9}$$

where C is the size of decomposed images, and s = 2 to length of C.

4 Proposed Technique

A new technique is proposed here using curvelet transform thresholding technique combined with the Wiener filter. The curvelet transform helps to overcome the problem of wavelet transform, and noise is removed using it first, and then, the Wiener filter is used to remove the residual noise.

5 Parameter Estimations

To evaluate the performance of the techniques, we have considered the values of peak signal-to-noise ratio (PSNR), mean square error (MSE), and structural similarity index measure (SSIM), which are defined by Eqs. (10), (11), and (12).

$$\mathrm{PSNR} = 10 \cdot \log_{10}\left(\frac{\mathrm{MAX}_I^2}{\mathrm{MSE}}\right) \tag{10}$$

$$\mathrm{MSE} = \frac{1}{mn}\sum_{i=0}^{m-1}\sum_{j=0}^{n-1}[f(i,j) - g(i,j)]^2 \tag{11}$$

where mn is size of image, MAX_I is maximum probable pixel value of the image, $f(i, j)$ is the noisy image, and $g(i, j)$ is denoised image.

$$\mathrm{SSIM}(x, y) = \frac{(2\mu_x\mu_y + C_1)(2\sigma_{xy} + C_2)}{(\mu_x^2 + \mu_y^2 + C_1)(\sigma_x^2 + \sigma_y^2 + C_2)} \tag{12}$$

where μ_x, μ_y are local means, σ_x, σ_y are standard deviations, and σ_{xy} is cross-covariance for images x, y.

6 Experimentation

In this work, the proposed technique along with other existing techniques is experimented on MRI images of brain. The experiments are performed using MATLAB on MRI images of size 256 × 256 following the wrapping technique on curvelet software package. White Gaussian noise is added in MRI images with different sigma, i.e., σ = 10, 20, 30, 40, 50, 60, 70. Then, the various types of denoising techniques were implemented, viz. Wiener filter, wavelet thresholding, curvelet thresholding, and curvelet thresholding, with Wiener filter.

7 Results and Discussion

After applying different denoising methods to noisy MRI brain image, results were compared visually and using quality metrics values of PSNR, MSE, and SSIM. The experimental results show that the proposed combined method of curvelet with Wiener filter-based image denoising is performed more effectively compared to other methods. Tables 1, 2 and 3 show the PSNR, MSE, and SSIM values obtained by each method for MRI brain image with different sigma, i.e., σ = 10, 20, 30, 40,

Table 1 Comparison of PSNR values for brain MRI image

Sigma σ	Wiener	Wavelet hard	Wavelet soft	Curvelet hard	Curvelet soft	Combined
10	31.452	29.198	28.154	30.351	28.153	42.179
20	26.611	23.952	23.529	24.336	23.011	43.364
30	23.708	20.875	20.686	20.932	20.050	44.630
40	23.708	18.743	18.660	18.608	17.978	45.943
50	19.849	17.064	17.037	16.829	16.400	47.543
60	18.456	15.729	15.718	15.462	15.133	48.500
70	17.297	14.590	14.583	14.318	14.057	50.421

Table 2 Comparison of MSE values for brain MRI image

Sigma σ	Wiener	Wavelet hard	Wavelet soft	Curvelet hard	Curvelet soft	Combined
10	46.550	78.219	99.460	59.973	99.496	3.937
20	141.890	261.756	288.531	239.570	325.069	2.997
30	276.860	531.575	555.183	524.607	642.812	2.239
40	276.860	868.621	885.359	895.977	1035.770	1.655
50	673.310	1278.371	1286.375	1349.516	1489.665	1.145
60	927.760	1738.323	1742.991	1848.875	1994.280	0.918
70	1211.600	2260.087	2263.393	2405.855	2554.956	0.590

Table 3 Comparison of SSIM values for brain MRI image

Sigma σ	Wiener	Wavelet hard	Wavelet soft	Curvelet hard	Curvelet soft	Combined
10	0.729	0.672	0.657	0.688	0.634	0.988
20	0.556	0.409	0.400	0.401	0.345	0.989
30	0.503	0.281	0.276	0.253	0.204	0.990
40	0.503	0.216	0.213	0.170	0.131	0.991
50	0.471	0.177	0.176	0.119	0.088	0.994
60	0.471	0.149	0.148	0.087	0.062	0.995
70	0.470	0.131	0.131	0.064	0.045	0.996

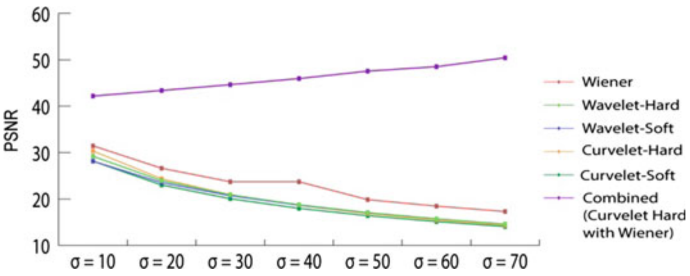

Fig. 1 PSNR values of MRI brain image

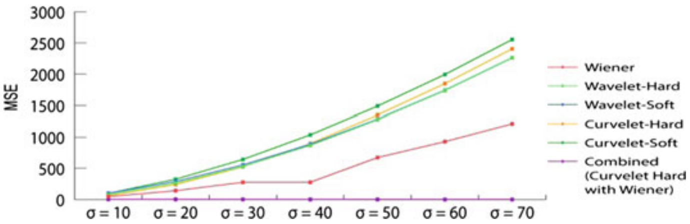

Fig. 2 MSE values of MRI brain image

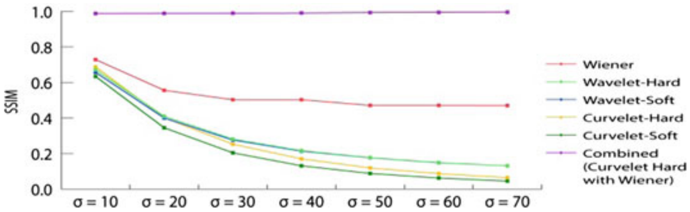

Fig. 3 SSIM values of MRI brain image

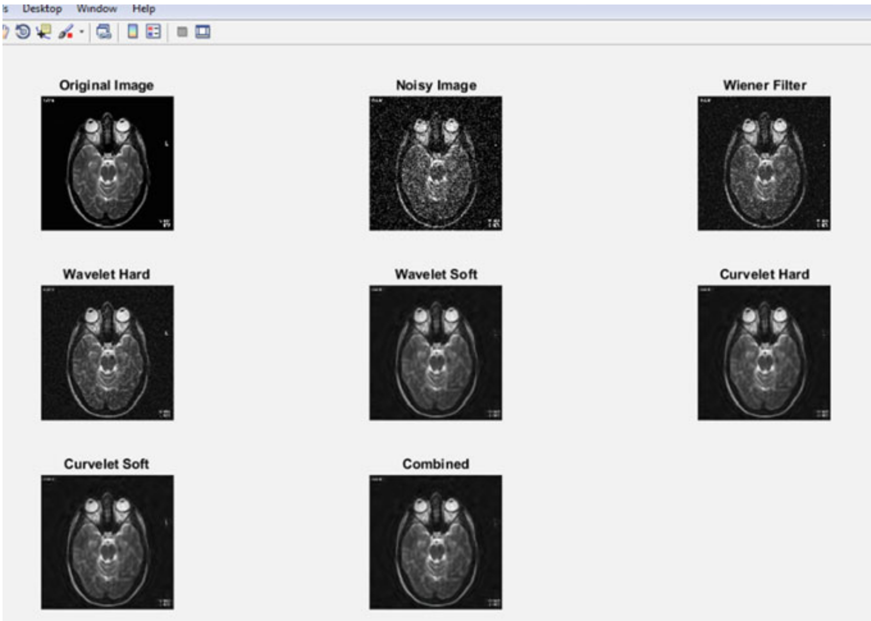

Fig. 4 Experimental results of MRI brain image denoising (where σ = 40)

50, 60, 70. The noise level of the image gradually comes down for the high PSNR value and the low MSE value. We have analysed that the combined method of curvelet with Weiner filter gives the higher PSNR and SSIM value and lower MSE value compared to other techniques. These are represented graphically in Figs. 1, 2, and 3, whereas in Fig. 4, the noisy image and resulting images of different methods corrupted by Gaussian noise with $\sigma = 40$ are shown. The visual quality of the image also becomes better in this combined curvelet with Wiener filter technique.

8 Conclusion

In this paper, we have studied wavelet, curvelet, and proposed filtering method and their effect in terms of the considered assessment parameters. The experimental results show that curvelet based approach performs better than the wavelet-based method. It also clearly indicates that curvelet with Wiener filter method outperforms compared to the other denoising methods, i.e., Wiener, wavelet, and curvelet. Also, the combined method does a very good job even when the noise is high as revealed from the experimental results. The curvelet denoising method removes the noise mostly lying in low frequency subbands, but some of the white Gaussian noise is spread in high frequency subbands also. So Weiner filter combined with curvelet transform is used here to remove that residual noise to some extent and the results were satisfactory.

References

1. Huang, T., Yang, G., Tang, G.: A fast two-dimensional median filtering algorithm. IEEE Trans. Acoust. Speech Signal Process. **27**(1), 13–18 (1979)
2. Ney, H.: A dynamic programming technique for nonlinear smoothing. In: IEEE International Conference on ICASSP, pp. 62–65 (1981)
3. Saluja, R., Boyat, A.: Wavelet based image denoising using weighted highpass filtering coefficients and adaptive wiener filter. In IEEE International Conference on Computer, Communication and Control (IC4-2015) (2015)
4. Boulfelfel, D., Rangayyan, R.M., Hahn, L.J., Kloiber, R.: Three dimensional restoration of single photon emission computed tomography images. IEEE Trans. Nucl. Sci. **41**(5), 1746–1754 (1994)
5. Lang, M., Guo, H., Odegard, J.E.: Noise reduction using an undecimated discrete wavelet transform. IEEE Signal Process. Lett. **3**, 10–12 (1995)
6. Chang, S.G., Yu, B., Vetterli, M.: Adaptive wavelet thresholding for image denoising and compression. IEEE Trans. Image Process **9**, 1532–1546 (2000)
7. Mojsilovic, A., Popovic, M., Sevic, D.: Classification of the ultrasound liver images with the 2nx1-d wavelet transform. In: Proceedings of IEEE International Conference Image Proceedings, vol. 1, pp. 367–370 (1996)
8. Donoho, D.L., Johnstone, I.M.: Ideal spatial adaptation via wavelet shrinkage. Biomefrika **81**, 425–455 (1994)
9. Donoho, D.L.: De-noising by soft thresholding. IEEE Trans. Inf. Theory **41**(3), 613–627 (1995)

10. Donoho, D.L., Johnstone, I.M.: Adapting to unknown smoothness via wavelet shrinkage. J. Am. Stat. Assoc. **90**, 1200–1224 (1995)
11. Stein, C.M.: Estimation of mean of a multivariate normal distribution. Ann. Stat. **9**, 1135–1151 (1981)
12. Zhang, X.: A denoising approach via wavelet domain diffusion and image domain diffusion. Multimedia Tools Appl. 1–17 (2016)
13. Candes, E.J., Donoho, D.L.: Ridgelets: a key to higher-dimensional intermittency? Phil. Trans. R. Soc. Lond. A **357**, 2495–2509 (1999)
14. Starck, J.L., Candes, E.J., Donoho, D.L.: The curvelet transform for image denoising. IEEE Trans. Image Process. **11**, 670–684 (2002)
15. Ulfarsson, M.O., Sveinsson, J.R., Benediktsson, J.A.: Speckle reduction of SAR images in the curvelet domain. In: Proceeding of the International Geoscience and Remote Sensing (IGARSS), vol. 1, pp. 315–317 (2002)
16. Liu, Y., Liu, Y.: Study on the basic principle and image denoising realization method of curvelet transform. In: International Conference on Multimedia Technology, pp. 1–4 (2010)
17. Ali, F.E., El-Dokany, I.M., Saad, A.A., El-Samie, F.E.A.: Fusion of MR and CT images using the curvelet transform. In: National Radio Science Conference, pp. 1–8 (2008). doi:10.1109/NRSC.2008.4542354
18. Candes, E.J., Demanet L., Donoho D.L., Ying, L. http://www.curvelet.org/